OXFORD

Cerebral Cortex, August 2020;30: 4438–4453

doi: 10.1093/cercor/bhaa033
Advance Access Publication Date: 7 March 2020
Original Article

ORIGINAL ARTICLE

Spatiotemporal Differences in the Regional Cortical Plate and Subplate Volume Growth during Fetal Development

Lana Vasung[1,2], Caitlin K. Rollins[3,4], Clemente Velasco-Annis[3], Hyuk Jin Yun[1,2], Jennings Zhang[1], Simon K. Warfield[3], Henry A. Feldman[2,5], Ali Gholipour[3,†] and P. Ellen Grant[1,2,†]

[1]Fetal-Neonatal Neuroimaging & Developmental Science Center (FNNDSC), Boston, MA 02115, USA, [2]Division of Newborn Medicine, Boston Children's Hospital, Harvard Medical School, Boston, MA 02115, USA, [3]Computational Radiology Laboratory, Boston Children's Hospital, Harvard Medical School, Boston, MA 02115, USA, [4]Department of Neurology, Boston Children's Hospital, Harvard Medical School, Boston, MA 02115, USA and [5]Institutional Centers for Clinical and Translational Research, Boston Children's Hospital, Harvard Medical School, Boston, MA 02115, USA

Address correspondence to Lana Vasung. Email: Lana.Vasung@childrens.harvard.edu
[†]Last co-authors.

Abstract

The regional specification of the cerebral cortex can be described by protomap and protocortex hypotheses. The protomap hypothesis suggests that the regional destiny of cortical neurons and the relative size of the cortical area are genetically determined early during embryonic development. The protocortex hypothesis suggests that the regional growth rate is predominantly shaped by external influences. In order to determine regional volumes of cortical compartments (cortical plate (CP) or subplate (SP)) and estimate their growth rates, we acquired T2-weighted in utero MRIs of 40 healthy fetuses and grouped them into early (<25.5 GW), mid- (25.5–31.6 GW), and late (>31.6 GW) prenatal periods. MRIs were segmented into CP and SP and further parcellated into 22 gyral regions. No significant difference was found between periods in regional volume fractions of the CP or SP. However, during the early and mid-prenatal periods, we found significant differences in relative growth rates (% increase per GW) between regions of cortical compartments. Thus, the relative size of these regions are most likely conserved and determined early during development whereas more subtle growth differences between regions are fine-tuned later, during periods of peak thalamocortical growth. This is in agreement with both the protomap and protocortex hypothesis.

Key words: cerebral cortex, fetus, gyrification, subplate, transient fetal compartments

Introduction

The cerebral cortex of the adult human brain displays striking regional nonuniformities in its cellular and subcellular organization. These differences were first studied histologically by examining cortical cytoarchitecture (the distribution of cells and their morphology in cortical layers), neuropil (distribution and density of synapses, dendrites, and axons in cortical layers), and myeloarchitecture (distribution and density of axonal myelin sheets within cortical layers (Brodmann 1909; Vogt 1910; Economo and Koskinas 1925; Vogt and Vogt 1926; Sanides

1964; Defelipe et al. 1999)). However, the lack of reproducibility of these studies, together with the technological advances, led researchers to develop more reliable measures. These measures include quantitative cytoarchitectonics (Zilles et al. 1979; Amunts et al. 1999; Palomero-Gallagher and Zilles 2018) and stereological approaches for mapping the receptor- and cytoarchitecture (Schleicher et al. 2000), immunohistochemical approaches (Smiley et al. 1994), and gene expression analyses (Hawrylycz et al. 2012). High-performance computing platforms, combined with high-performance data analytics, allowed us today to obtain high-resolution maps of the cerebral cortex (Amunts et al. 2013) and to create probabilistic cytoarchitectonic and receptor maps in a large number of subjects (Amunts and Zilles 2015; Eickhoff et al. 2005). Yet, in contrast to the adult human cerebral cortex, very little is known about the changes in cortical architecture that occur during in utero development.

During embryonic and early fetal development, the cerebral cortex contains relatively uniform neuropil and densely packed post-migratory neurons that are of similar size and shape across regions (Bayer and Altman 2005, 2007; Judaš et al. 2006; Kostović et al. 2008a). Thus, although little has been known about how the areal differences of cortex emerge during prenatal brain development, regional changes in cortical volume can be used to infer regional differences in neuronal density and their maturation.

Basic science research suggests that two theories can be used in order to characterize the arealization of the cerebral cortex during development: the protomap and the protocortex hypothesis. According to the protomap hypothesis, the regional identity of neuronal precursors is determined by their localization in the ventricular zone (Rakic 1988; Rubenstein and Rakic 1999; Bishop et al. 2000). In contrast, the protocortex hypothesis argues that the regional identity of neurons is achieved by cortical ingrowth of fibers, most notably by the density of the thalamocortical input, which carries the extrinsic signal to the cortex (Van der and Woolsey 1973; Creutzfeldt 1977; O'Leary 1989). Experimental models in animals suggest that these two theories should be unified (for an extensive review, see (Cadwell et al. 2019)). However, to our knowledge there has been little evidence coming from in vivo human neuroimaging studies that supports these two theories. In addition, the differential growth of cortical fetal compartments (i.e., cortical plate (CP) and subplate (SP)) during the peak growth of thalamocortical fibers might result in biomechanical forces driving the cortical folding (Kostovic and Rakic 1990; Ronan and Fletcher 2015). However, to our knowledge, there is no data in the prenatal human brain that has tested the feasibility of these theories.

The introduction of neuroimaging methods during the twenty-first century has transformed the way we understand and study the human cerebral cortex. Although we still rely on landmark-based gyral cortical maps (Desikan et al. 2006), techniques such as high-resolution magnetic resonance imaging (MRI) have enabled us to visualize regional cortical differences during different stages of life, but still at a much lower spatial scale in comparison to histology (Raznahan et al. 2011; Khundrakpam et al. 2015; Lyall et al. 2015; Ducharme et al. 2016; Tamnes et al. 2017)). Furthermore, in recent years there has been an increasing amount of literature addressing the association of regional changes of the cerebral cortex with environmental and genetic influences (for review see (Thompson et al. 2017)), adverse intrauterine environmental factors, and premature birth. Nonetheless, despite the growing knowledge about cortical maturation, the trajectories of regional cortical expansion during normal in utero development remain largely unknown.

In this study, we used in vivo fetal brain MRIs in order to identify regional differences in the volume expansion of the fetal cortex during in utero development. The fetal cortex is composed out of two main transient compartments: the SP and the CP (Kostovic and Rakic 1990;Bystron et al. 2008). Both transient compartments can be reliably identified by in vivo MRI (Kostović et al. 2002; Rados et al. 2006; Gholipour et al. 2014; Gholipour et al. 2017; Diogo et al. 2019). However, during development, the spatiotemporal appearance and morphology of sulci varies between individuals (Chi et al. 1977; Ono et al. 1990; Garel et al. 2001; Germann et al. 2005; Iaria and Petrides 2007; Zlatkina and Petrides 2010; Habas et al. 2012; Segal and Petrides 2012; Yun et al. 2018). Fetal cortical surface templates with parcellated regions are currently unavailable. In light of this, we manually parcellated the fetal cortex of each brain into 22 gyral regions (Fig. S1) following the anatomical landmarks that were described in adults. (ten Desikan et al. 2006; Donkelaar et al. 2018).

Our null hypothesis was that there are no significant differences between periods in volume fractions of CP or SP regions with respect to the total volume of the CP or SP. This hypothesis is in agreement with the protomap hypothesis (the CP or SP areal destiny and size are determined early during fetal development). Our second hypothesis was that within periods there are significant differences in the relative growth rate (i.e., percent increase per GW) between neighboring regions. This is in agreement with the protocortex hypothesis. Thus, for the purpose of our study, based on the descriptions of major histogenic processes in the human (Bystron et al. 2008; Kostovic and Vasung 2009; Clowry et al. 2010; Molnár and Hoerder-Suabedissen 2016; Vasung et al. 2018) and their gestational age, we divided the fetuses in three prenatal periods: early, mid-, and late prenatal period. The early prenatal period (<25.5 gestational weeks (GW), or < 23.5 post-conceptual weeks (PCW)), is characterized by the accumulation of thalamocortical fibers in the SP (Clowry et al. 2010; Krsnik et al. 2017). The mid-prenatal period (25.5–31.6 GW, or 23.5–29.6 PCW) is characterized by the ingrowth of thalamocortical fibers in the CP (Krsnik et al. 2017) and by the appearance of sulcal roots (Chi et al. 1977; Yun et al. 2018). Finally, the late prenatal period (>31.6 GW, or > 29.6 PCW) is characterized by laminar differentiation of the CP and by the emergence of the six-layered cortical pattern (Kostović et al. 2008b; Kostovic and Vasung 2009; Krsnik et al. 2017).

The rationale of our work was to gain insight and provide information on the relative growth of CP and SP, as well as differential growth of neighboring CP and SP regions, that are comparable to the regions widely used for studying children, adolescents, and adults (Desikan et al. 2006).

Materials and Methods

Materials

In a study approved by the local Institutional Review Board Committee, we acquired in vivo MRIs of 40 healthy fetuses (16.43–36.86 GW, 15 females, Fig. S2). The protocol involved multiple T2-weighted (T2w) half-Fourier single shot turbo spin echo (HASTE) scans (TR = 1400–2000 ms, TE = 100–120 ms, voxel size = 0.9x1.1x2mm^3) in the axial, coronal, and sagittal planes with respect to the fetal brain, on a 3-T Siemens Skyra MRI scanner. Based on gestational age at scan time, the fetuses were

grouped into three prenatal periods: early (<25.5 GW, $N = 14$), mid- (25.5–31.6 GW, $N = 11$), and late (>31.6 GW, $N = 15$).

Methods

MRI Preprocessing

Fetal MRIs were preprocessed using the in-house-built fetal pipeline ((Gholipour et al. 2017), Fig. S3). First, the fetal MRIs were motion-corrected, reconstructed in 3D, and resampled to an isotropic resolution (Kainz et al. 2015). Next, the fetal brains were masked (Salehi et al. 2017), the bias field was corrected, and intensities were normalized using N4 (Tustison et al. 2010). In the final step, the fetal brains were registered to a spatiotemporal fetal brain MRI atlas (Gholipour et al. 2017).

Parcellation of the CP and SP

The preprocessed MRI images were further processed using the in-house-built pipeline which is composed of the following steps (for details see (Vasung et al. 2016, Vasung et al. 2019)): (1) automatic multi-atlas-based segmentation of the CP and SP ((Gholipour et al. 2017), Fig. S4), (2) manual refinement of the segmented compartments according to the histological and MRI guidelines ((Išasegi et al. 2018; Vasung et al. 2019), Fig. S4), (3) surface extraction of the segmented CP and SP ((Vasung et al. 2016, 2019), Fig. S5), (4) manual parcellation of 24 regions of interest (Fig. S1A, Fig. S1B, and Fig. S5) according to the Desikan-Killiani atlas (Desikan et al. 2006) but taking into consideration the appearance of the gyri and sulci (Chi et al. 1977; Garel et al. 2001; Habas et al. 2012; Yun et al. 2018), (5) projection of surface labels to the underlying CP and SP voxels (Fig. S5), and (6) co-registering the projected regions in volumetric space with the initially segmented CP or SP mask (Avants et al. 2011). Given the considerable variation in the visibility and appearance of sulci dividing some of the regions the fusiform, middle and inferior temporal gyri and the temporal pole were grouped together into one region called latero-inferior temporal neocortex (for details see Vasung et al. 2019). As a result, statistical analyses were performed using 22 regions of CP and SP.

Statistical Analysis

Between period analyses. First, we calculated the regional volume (V) fraction of the CP and SP for each subject, with respect to the total volume of the CP or SP, where the VCP_fraction $= \frac{V[CPregional]}{V[CP\ total]} \times 100$ and the VSP_fraction $= \frac{V[SPregional]}{V[SP\ total]} \times 100$.

The mean volume fractions of the CP and SP for each region were compared between periods using a student's t-tests. We hypothesized that the regional CP or SP volumes, in comparative relation to the total CP or SP volume, will be similar between periods that is in agreement with the protomap hypothesis.

Within period analyses. Next, we conducted an analysis to identify differences between neighboring regions (example in Fig. S1C) in their relative growth rate during each period (% increase per GW). We hypothesized that differences in regional growth rates of CP or SP within periods would be significantly different between neighboring regions, consistent with the protocortex hypothesis.

We identified 60 pairs of neighboring regions in which we estimated and compared volumetric growth rates (an example of four pairs of regions for the inferior frontal gyrus is shown in Fig. S1C). We conducted separate analyses for the CP and SP during early (<25.5 GW), mid- (25.5–31.6 GW), and late (>31.6 GW) prenatal periods. Owing to incomplete data (e.g., SP zone was not identified as a continuous zone after 32 GW (Vasung et al. 2019)), we were able to produce 300 of the total 360 possible analyses. All regional volumes exhibited skewed distributions and were log-transformed for analysis.

For each pair of neighboring regions, we constructed a repeated measures linear model for log volume as a function of age in GW (measured continuously) with adjustment for sex and hemisphere. An interaction term was included to provide region-specific GW coefficients. We used an unstructured Kronecker product covariance matrix to account for heterogeneous variance and correlation among the two regions and two hemispheres measured on each fetus. To reduce the influence of extreme values, we applied an iterative algorithm for detecting and deleting outliers, equivalent to robust regression with M-estimation (Holland and Welsch 1977). The fitted region-specific coefficients of GW (b) were retransformed to yield estimates of the region-specific growth rates (100% × (exp(b)—1)), and their difference (Δb) was similarly retransformed to yield an estimate of the percentage difference in growth rates between the two neighboring regions.

The standard error of each measurement was estimated, enabling us to test each of the 300 pairs of regions for a significant difference in growth rate. We applied the Holm step-down procedure to enforce a familywise Type I error rate of 5%, that is, < 5% chance of making even one false declaration of significance among the 300 comparisons (Holm 1979). We estimated the false discovery rate to be 0.28% for the set of 18 regional differences declared significant (Benjamini and Yekutieli 2001), that is, the probability that at least one difference declared significant would, in fact, be null. We used SAS software (version 9.4, Cary, NC) for all computations.

Results

Volume Fractions of CP and SP Are Not Significantly Different between Periods

We did not find significant differences between periods in the regional volume fractions of the CP and SP ($P > 0.05$, Fig. 1, Table S1, Table S2).

Early and Mid-prenatal Periods Are Characterized by Asynchronous Growth of CP and SP

Global Asynchrony in Relative Growth of CP and SP

We observed variations in relative volume growth (% per GW) of the CP (Fig. 2) and SP (Fig. 3) during the early and mid-prenatal periods (Table 1, Table 2). This was not observed during the late prenatal period (Table 3).

During the early period, the cuneus, precentral, supramarginal, lingual, orbitofrontal cortex, and superior temporal gyrus increased more than a quarter of their volume with each GW. All other CP regions increased less than a quarter per GW (Fig. 2A, Fig. 2D, and Table 1).

During the mid-prenatal period, the relative increase of CP regions per GW was more pronounced. Almost 30% of regions increased less than a quarter per GW, 30% of regions increased more than a quarter, and the cingulate gyrus, gyrus rectus, paracentral lobule, and inferior parietal cortex increased more than a third with each GW (Fig. 2B, Fig. 2E, and Table 2).

In contrast to the CP, the relative volume increase of the SP per GW was more pronounced during the early period. During the early period (<25.5 GW), the SP increased in almost all segmented regions (except inferior frontal gyrus and superior

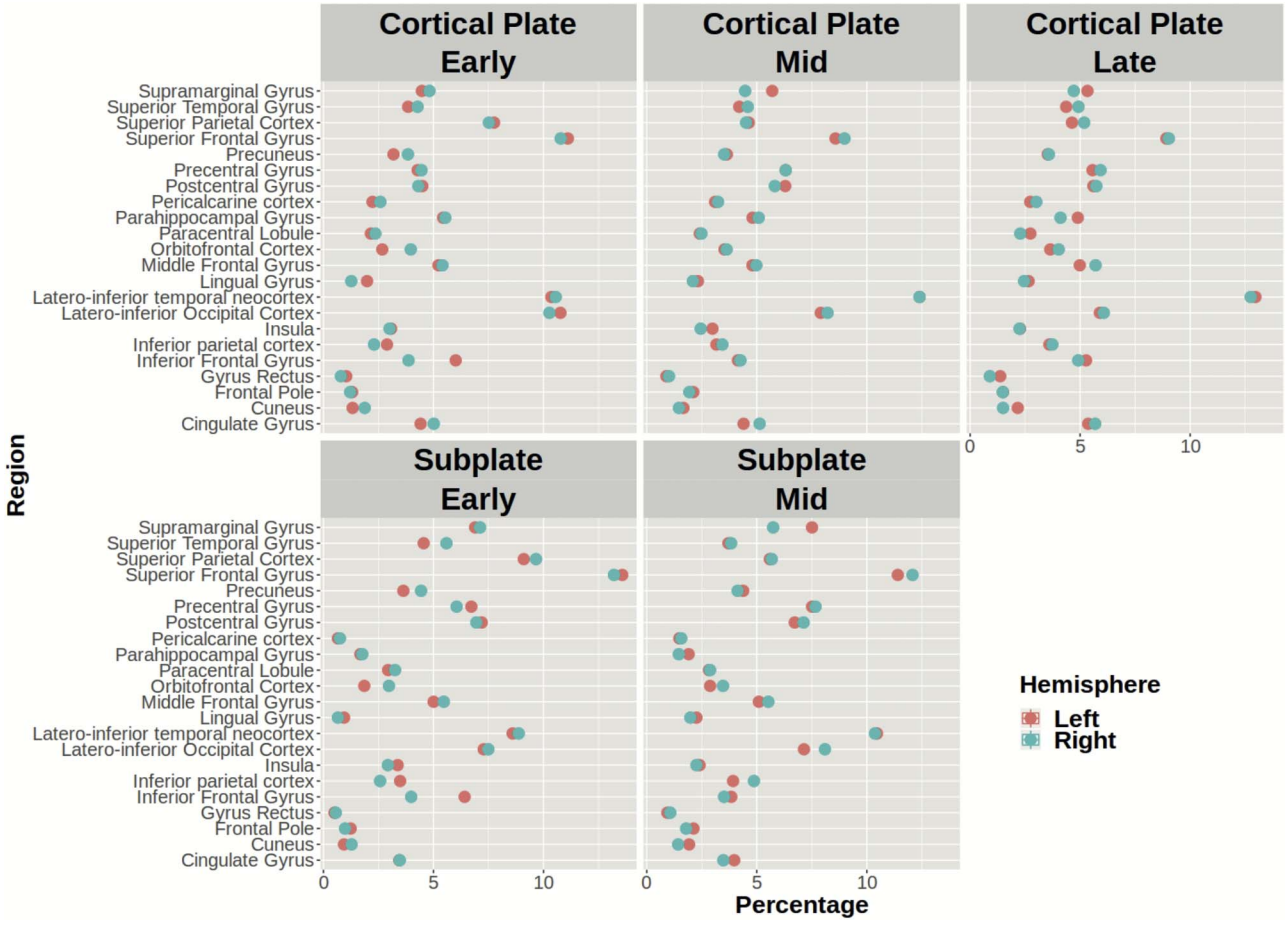

Figure 1. The average regional volume fraction of the CP (*upper row*) and SP (*lower row*) in the left (*red circle*) and right hemisphere (*blue circle*) during early, mid-, and late prenatal periods. Note that the mean volume percentage of CP and SP for each region is similar across periods.

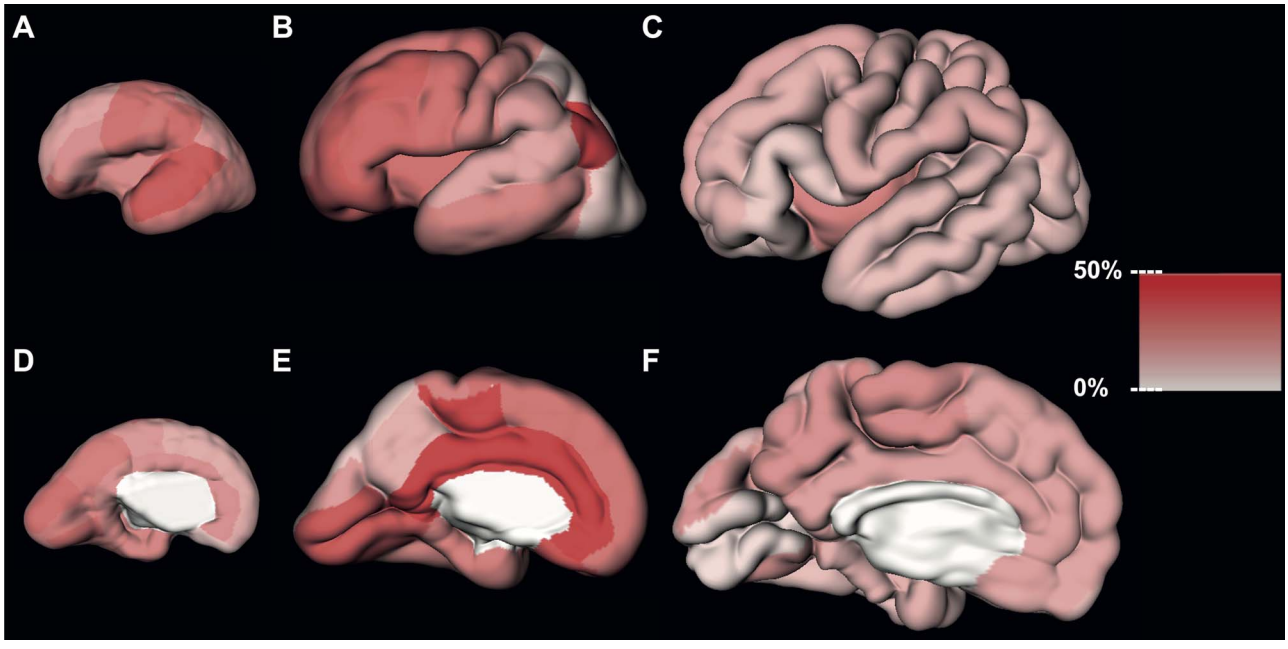

Figure 2. Estimated regional volume growth of the CP during early (*first column*), mid- (*second column*), and late (*third column*) prenatal periods.

Table 1 Regional increase in the volume (percentage per GW) of the CP and SP during the early prenatal period (<25.5 GW)

Region	Fetal compartment	Increase per GW (%)	95% CI (min, max)		Relative fraction increase	Fetal compartment	Increase per GW (%)	95% CI (min, max)		Relative volume fraction increase
Gyrus rectus	Cortical plate	8.10	−2.44	19.80	<Quarter	Subplate	61.91	37.79	90.37	>third
Superior frontal gyrus	Cortical plate	12.56	7.71	17.63	<Quarter	Subplate	33.03	25.15	41.41	>Third
Frontal pole	Cortical plate	14.30	5.71	23.58	<Quarter	Subplate	38.81	25.39	53.70	>Third
Middle frontal gyrus	Cortical plate	14.56	9.38	19.99	<Quarter	Subplate	26.52	17.92	35.75	>Quarter
Superior parietal lobule	Cortical plate	16.06	10.97	21.39	<Quarter	Subplate	26.47	20.80	32.41	>Quarter
Paracentral lobule	Cortical plate	16.54	12.56	20.66	<Quarter	Subplate	32.66	26.43	39.20	>Quarter
Inferior parietal cortex	Cortical plate	17.06	11.31	23.11	<Quarter	Subplate	27.31	21.37	33.53	>Quarter
Cingulate gyrus	Cortical plate	18.26	12.90	23.87	<Quarter	Subplate	66.65	52.36	82.31	>Third
Inferior frontal gyrus	Cortical plate	18.78	11.77	26.23	<Quarter	Subplate	20.57	11.80	30.02	<Quarter
Insula	Cortical plate	19.92	13.58	26.63	<Quarter	Subplate	33.96	23.74	45.04	>Third
Lateral occipital cortex	Cortical plate	20.17	15.86	24.65	<Quarter	Subplate	35.30	27.55	43.55	>Third
Parahippocampal gyrus	Cortical plate	20.77	15.88	25.87	<Quarter	Subplate	98.61	78.08	121.59	>Third
Pericalcarine cortex	Cortical plate	21.95	15.99	28.22	<Quarter	Subplate	35.13	20.21	51.99	>Third
Precuneus	Cortical plate	22.50	17.13	28.11	<Quarter	Subplate	37.10	31.09	43.38	>Third
Latero-inferior temporal cortex	Cortical plate	23.01	17.85	28.41	<Quarter	Subplate	39.16	32.04	46.66	>Third
Postcentral gyrus	Cortical plate	23.89	18.89	29.11	<Quarter	Subplate	26.25	21.12	31.60	>Quarter
Precentral gyrus	Cortical plate	25.51	20.32	30.93	>Quarter	Subplate	29.55	22.34	37.19	>Quarter
Cuneus	Cortical plate	25.89	17.97	34.34	>Quarter	Subplate	48.41	36.04	61.97	>Third
Supramarginal gyrus	Cortical plate	26.41	20.05	33.10	>Quarter	Subplate	29.05	22.12	36.39	>Quarter
Orbitofrontal cortex	Cortical plate	26.43	18.19	35.26	>Quarter	Subplate	47.27	40.07	54.84	>Third
Lingual gyrus	Cortical plate	26.79	18.23	35.97	>Quarter	Subplate	63.08	39.51	91.08	>Third
Superior temporal gyrus	Cortical plate	31.96	25.71	38.52	>Quarter	Subplate	22.54	16.85	28.51	<Quarter

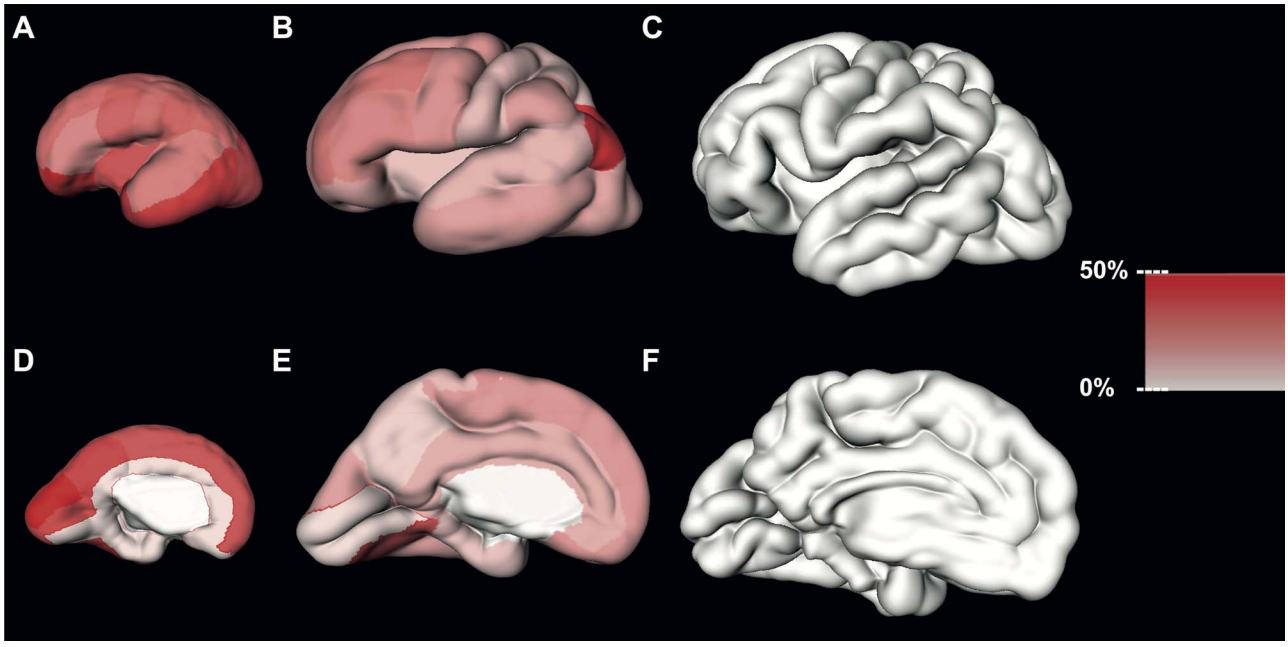

Figure 3. Estimated regional volume growth of the SP during early (*first column*), mid- (*second column*), and late (*third column*) prenatal periods.

temporal gyrus) at least one-quarter of the volume per each GW (Fig. 3A, Fig. 3D, and Table 1). Furthermore, almost half of segmented regions increased by at least one-third of their volume with each GW (the average relative volume increase of SP ranged from 33.03% to 98.61% per GW (Fig. 3A, Fig. 3D, and Table 1)).

During the mid-prenatal period, with each GW almost all regions of the SP increased less than a quarter of their volume. The lingual gyrus, inferior parietal cortex, and pericalcarine cortex increasing by at least one-third of their initial volumes (Fig. 3B, Fig. 3E, and Table 2).

Local Asynchrony in Relative Growth of CP and SP between Neighboring Regions

We observed significant differences in volume growth (average % increase per GW) between neighboring regions of the CP during early and mid-prenatal periods (Fig. 4).

The relative volume increase of the superior frontal gyrus was significantly slower compared to the relative volume increase of the precentral gyrus [mean difference = −10.85%, 95% confidence interval (CI) (−15.65, −5.78)] during the early period (Table 4, Fig. 4A and *D*).

During the mid-prenatal period, the relative volume increase per GW of the lateral occipital cortex [mean difference = −21.28%, 95% CI (−27.35,-14.70)], superior temporal gyrus [mean difference = −18.36%, 95% CI (−24.69,-11.51)], and superior parietal lobule [mean difference = −21.44%, 95% CI (−28.26,-13.96)] was significantly slower compared to the inferior parietal cortex (Table 5, Fig. 4B). Furthermore, during the mid-prenatal period, the relative volume increase of the lateral occipital cortex was significantly slower compared to the increase of the latero-inferior temporal cortex [mean difference = −10.75%, 95% CI (−15.12,-6.16), Table 5, Fig. 4E]. Similar differences were observed between paracentral lobule and precuneus with precuneus showing significantly slower growth [mean difference = −17.67%, 95% CI (−24.77, −9.96), Table 5, Fig. 4E].

We observed significant differences in relative volume increase (average % increase per GW) of neighboring regions of the SP during early and mid-prenatal periods (Table 4, Table 5, Fig. 5).

Compared to the latero-inferior temporal cortex, the relative volume increase during the early period was significantly slower for the superior temporal gyrus [mean difference = −10.99%, 95% CI (−15.77, −5.94)] and the inferior parietal cortex [mean difference = −11.50%, 95% CI (−16.04, −6.72), Table 4, Fig. 5A]. Furthermore, the superior parietal lobule volume increase was also significantly slower compared to the cuneus [mean difference = −16.11%, 95% CI(−22.44, −9.26), Table 4, Fig. 5A]. During the early period, significant differences were also observed between limbic regions. Compared to the cingulate gyrus during the early period, relative volume increase was significantly slower in the superior frontal gyrus [mean difference = −23.54%, 95% CI (−29.54,-17.07), Table 4, Fig. 5C], paracentral lobule [mean difference = −23.15%, 95% CI (−28.21, −17.74), Table 4, Fig. 5C], and precuneus [mean difference = −14.49%, 95% CI (−20.46,-8.07), Table 4, Fig. 5C]. In comparison to the parahippocampal gyrus, significantly slower volume increase was found in the insula [mean difference = −34.68%, 95% CI (−41.14,-27.51), Table 4, Fig. 5C], pericalcarine cortex [mean difference = −29.17%, 95% CI (−35.45,-22.27), Table 4, Fig. 5C], and latero-inferior temporal cortex [mean difference = −29.27%, 95% CI (−37.76,-19.61), Table 4, Fig. 5C].

During the mid-prenatal period, compared to the inferior parietal cortex, the relative volume increase was significantly slower in superior temporal gyrus [mean difference = −22.47%, 95% CI (−30.68,-13.27), Table 5, Fig. 5B] and latero-inferior temporal cortex [mean difference = −18.85%, 95% CI (−26.09,-10.87), Table 5, Fig. 5B]. Lastly, compared to the growth of the pericalcarine cortex, the relative volume growth of the precuneus was significantly slower [mean difference = −30.56% slower, 95% CI (−40.66,-18.73), Table 5, Fig. 5D].

Table 2 Regional increase in the volume (percentage per GW) of the CP and SP during the mid-prenatal period (25.5–31.6 GW)

Region	Fetal compartment	Increase per GW (%)	95% CI (min, max)		Relative fraction increase	Fetal compartment	Increase per GW (%)	95% CI (min, max)		Relative fraction increase
Superior parietal lobule	Cortical plate	7.74	−2.89	19.58	<Quarter	Subplate	8.36	−1.34	19.02	<Quarter
Lateral occipital cortex	Cortical plate	7.88	2.57	13.48	<Quarter	Subplate	14.08	4.23	24.87	<Quarter
Precuneus	Cortical plate	12.31	1.60	24.16	<Quarter	Subplate	6.87	−1.44	15.88	<Quarter
Superior temporal gyrus	Cortical plate	14.35	5.59	23.84	<Quarter	Subplate	11.56	3.67	20.05	<Quarter
Supramarginal gyrus	Cortical plate	15.76	7.58	24.56	<Quarter	Subplate	16.23	5.49	28.06	<Quarter
Cuneus	Cortical plate	16.32	0.80	34.29	<Quarter	Subplate	14.79	−1.24	33.59	<Quarter
Latero-inferior temporal cortex	Cortical plate	20.93	11.41	31.27	<Quarter	Subplate	15.43	7.42	24.04	<Quarter
Postcentral gyrus	Cortical plate	21.58	14.28	29.36	<Quarter	Subplate	10.42	0.18	21.71	<Quarter
Parahippocampal gyrus	Cortical plate	22.29	15.46	29.54	<Quarter	Subplate	8.82	−5.06	24.78	<Quarter
Superior frontal gyrus	Cortical plate	24.18	16.29	32.61	<Quarter	Subplate	16.60	8.36	25.46	<Quarter
Precentral gyrus	Cortical plate	25.82	18.11	34.03	>Quarter	Subplate	18.20	10.08	26.93	<Quarter
Insula	Cortical plate	26.27	15.12	38.51	>Quarter	Subplate	9.10	−1.10	20.38	<Quarter
Inferior frontal gyrus	Cortical plate	27.99	20.21	36.28	>Quarter	Subplate	20.76	13.63	28.33	<Quarter
Middle frontal gyrus	Cortical plate	30.09	18.92	42.32	>Quarter	Subplate	24.76	6.97	45.53	<Quarter
Orbitofrontal cortex	Cortical plate	30.21	17.38	44.47	>Quarter	Subplate	13.84	1.77	27.37	<Quarter
Frontal pole	Cortical plate	31.09	13.53	51.40	>Quarter	Subplate	12.00	−0.31	25.91	<Quarter
Lingual gyrus	Cortical plate	31.78	17.82	47.42	>Quarter	Subplate	33.44	12.79	57.91	>Third
Pericalcarine cortex	Cortical plate	32.25	19.12	46.82	>Quarter	Subplate	60.09	34.06	91.35	>Third
Gyrus rectus	Cortical plate	33.17	16.96	51.69	>Third	Subplate	17.53	3.50	33.51	<Quarter
Paracentral lobule	Cortical plate	37.25	27.44	47.83	>Third	Subplate	16.25	3.46	30.71	<Quarter
Cingulate gyrus	Cortical plate	38.30	24.83	53.24	>Third	Subplate	12.22	−0.89	27.13	<Quarter
Inferior parietal cortex	Cortical plate	38.33	27.68	49.88	>Third	Subplate	42.90	28.22	59.28	>Third

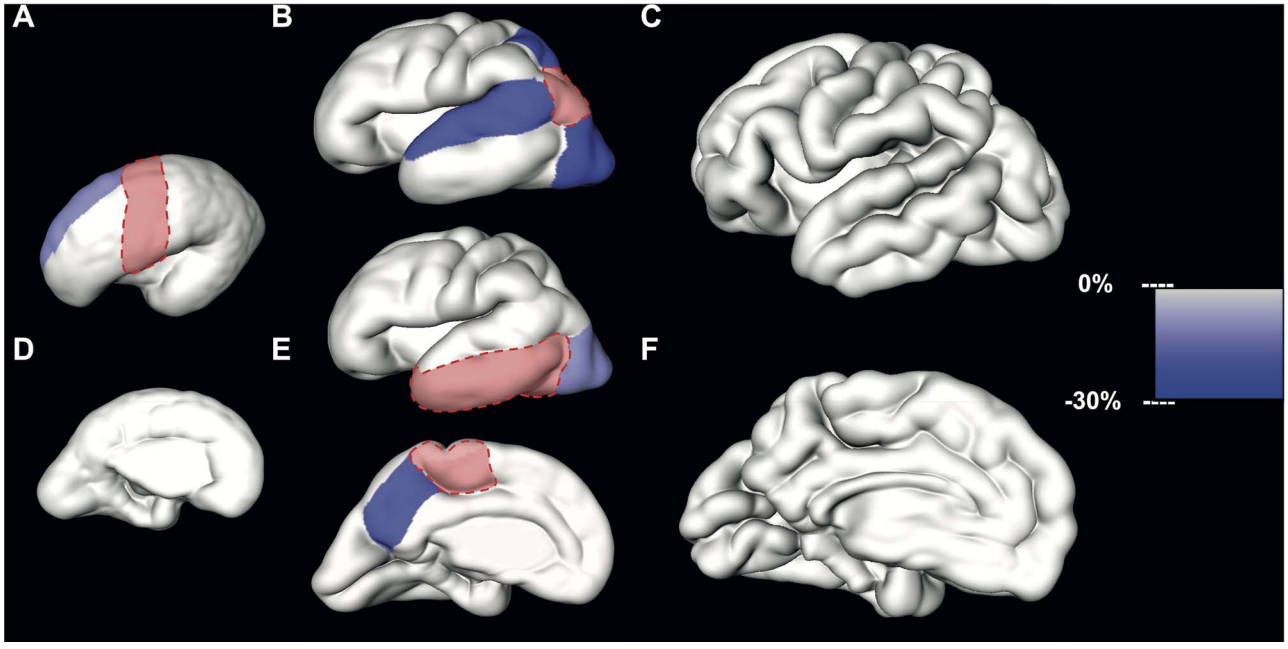

Figure 4. Significant differences in relative volume increase (average % increase per GW) of neighboring CP regions during early (*first column*), mid- (*second column*), and late (*third column*) prenatal periods. The slower growth rate per GW of regions neighboring the reference region (*in red*) is color-coded (*right scale bar*) and superimposed to the reconstructed lateral or medial CP surface.

Late Prenatal Period Is Characterized by Synchronous Growth of CP

During the late period, the relative growth rate of CP per GW was similar between regions, that is, per GW they increased less than a quarter (Fig. 2C, Fig. 2F, Table 3). Furthermore, no significant difference in relative volume increase between neighboring regions of CP was observed during the late preterm period (Fig. 4C and Fig. 4F).

Discussion

To our knowledge, this is the first study to address volume fractions of CP and SP regions, the relative growth of CP and SP regions, as well as regional differences between neighboring regions in CP and SP growth during in utero human brain development. This study showed three major results: (i) lack of significant differences in the regional volume fractions of the CP or SP between early, mid-, and late prenatal periods; (ii) asynchronous regional growth (percent increase) of CP and SP during early and mid-prenatal periods, that is, the periods of peak gyrification; and (iii) synchronous growth of CP during the late prenatal period.

Similarities in Regional Volume Fractions of CP and SP during Early, Mid-, and Late Prenatal Periods

Our null hypothesis was that the volume partition of CP or SP regions is conserved during the preterm development. We failed to find significant differences between periods in relative volumes of CP and SP. This is in agreement with the protomap hypothesis suggesting that the relative size of the CP and SP regions is determined early during prenatal development.

Neuronal progenitors that are situated in the proliferative zones lining the ventricles (ganglionic eminence, ventricular zone, and subventricular zone) form a mosaic of proliferative units that are patterned by gradients of transcription factors (Rubenstein et al. 1998; O'Leary and Nakagawa 2002; Bayatti et al. 2008; Mallamaci and Stoykova 2006). This arrangement of progenitor cells leads to the establishment of their regional identity, which has been described as a "protomap" of the future cortex (Rakic 1988). The migration of neuronal precursors from proliferative zones to their final destination in the CP occurs predominantly between 8 and 26 GW (Meyer 2007; Bystron et al. 2008; Workman et al. 2013). Given that most of those migrating neuronal precursors are destined to become glutamatergic neurons, they migrate radially, that is, via glial scaffold, retaining their regional identity (Rakic and Sidman 1968). By 26 GW, the majority of glutamatergic neurons have already reached their final destination in the CP (Bystron et al. 2008). After 26 GW, and until early postnatal periods, only a small portion of neurons, predominantly GABAergic, continue to migrate tangentially (Xu et al. 2011; Paredes et al. 2016). Thus, basic neuroscience provided evidence that during the early prenatal period (<25.5 GW), the CP contains predominantly tightly packed post-migratory neurons that are arranged into radial ontogenic columns (Rakic 1988). In-line with the aforementioned, it can be inferred that later on during the mid- (25.5–31.6 GW) and late (>31.6 GW) prenatal periods, the number of post-migratory neurons in cortical regions will remain similar. Therefore, it is likely that an increase in the absolute volume of the cortical region will be predetermined by its initial size and the number of neurons preserving relative regional volume fractions of the CP or SP across development.

Additionally, experimental models in animals indicate that the overall size of neocortex does not change after bilateral enucleation (i.e., loss of thalamocortical input, (Karlen and Krubitzer

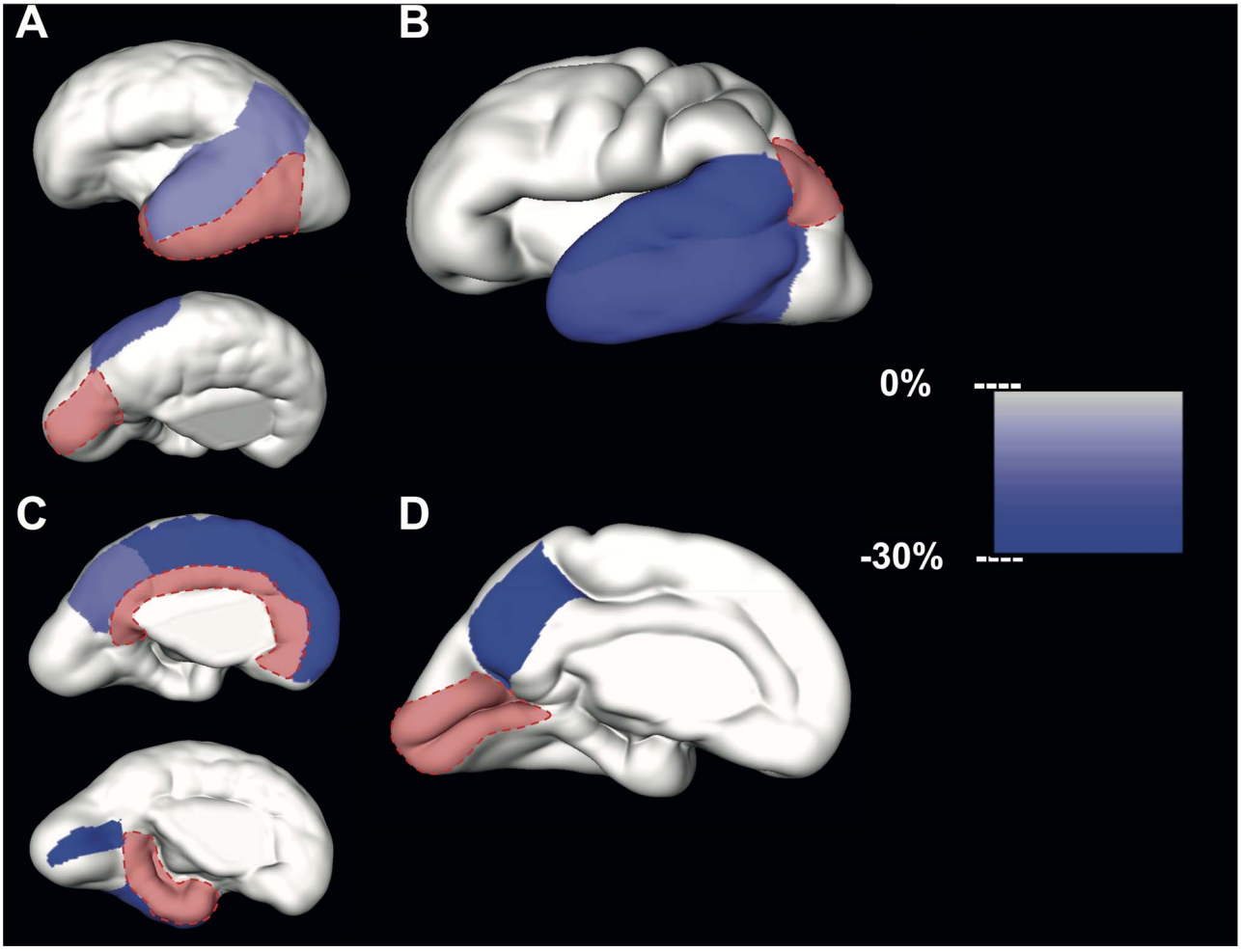

Figure 5. Significant differences in relative volume increase (average % increase per GW) of neighboring SP regions during early (*first column*) and mid- (*second column*) prenatal periods. The slower growth rate per GW of regions neighboring the reference region (*in red*) is color-coded (*right scale bar*) and superimposed to the reconstructed lateral and medial CP surfaces. Note that after 32 GW SP could not be identified as a continuous compartment.

2009)). What changes is the percentage of the neocortex devoted to the primary visual or somatosensory area (Rakic et al. 1991; Karlen and Krubitzer 2009).

Taking all together, our results are in agreement with the protomap hypothesis, which suggests that the regional destiny of cortical neurons and the relative size of the cortical area are genetically determined early during embryonic development (Rakic 1988; Rakic et al. 1991). However, we acknowledge that with the current methodology we cannot test this causal relationship.

Early and Mid-prenatal Periods Are Characterized by Asynchronous Growth of CP and SP Regions Which Parallels the Emergence of Cortical Folds

The similar volume fractions of the CP and SP regions between prenatal periods do not translate to similar regional growth rates within periods. It is the opposite. As expected, our results show variation in the relative regional volume increase of the CP and SP during the early and mid-prenatal periods.

During Early and Mid-prenatal Periods, the Growth of CP and SP Regions Is Globally Asynchronous

Although the microstructural substrate for differences between regions in the volume expansion is unknown, several studies suggest that the speed and the amount of the cortical expansion might be related to cellular and subcellular complexity (Chenn and Walsh 2002; Hill et al. 2010). The differences in cytoarchitecture, neuropil, and myeloarchitecture between certain brain regions of the adult human brain are known. For example, in the adult brain, the lateral temporal cortex (Brodmann area 21) has twofold greater dendritic field areas compared to the lateral occipital cortex (Brodmann area 18) (Elston et al. 2001). By the same token, today we can characterize differences between regions in their maturation speed. For example, adult levels of mean cortical thickness, gray matter density, and synaptic density are reached earlier in pericalcarine cortex, calcarine cortex, and Heschl's gyrus compared to the dorsolateral and parietal cortices (Huttenlocher and Dabholkar 1997; Toga et al. 2006; Shaw et al. 2008). In this context, our results also indicate a differential growth and maturation of cortical regions. Moreover, they are in agreement with the work

Table 3 Regional increase in the volume (percentage per GW) of the CP during the late prenatal period (>31.6 GW)

Region	Fetal compartment	Increase per GW (%)	95% CI (min, max)		*Relative fraction increase*
Pericalcarine cortex	Cortical plate	4.84	−1.13	11.17	<Quarter
Inferior frontal gyrus	Cortical plate	7.47	−0.63	16.23	<Quarter
Orbitofrontal cortex	Cortical plate	8.28	1.51	15.51	<Quarter
Latero-inferior temporal cortex	Cortical plate	9.51	4.82	14.40	<Quarter
Lateral occipital cortex	Cortical plate	9.78	4.42	15.41	<Quarter
Superior temporal gyrus	Cortical plate	10.37	3.34	17.87	<Quarter
Frontal pole	Cortical plate	10.47	1.11	20.71	<Quarter
Middle frontal gyrus	Cortical plate	11.61	5.32	18.28	<Quarter
Inferior parietal cortex	Cortical plate	11.76	4.59	19.43	<Quarter
Postcentral gyrus	Cortical plate	11.82	6.87	17.01	<Quarter
Precentral gyrus	Cortical plate	12.07	6.07	18.42	<Quarter
Parahippocampal gyrus	Cortical plate	12.21	6.86	17.83	<Quarter
Superior parietal lobule	Cortical plate	12.95	8.13	17.98	<Quarter
Supramarginal gyrus	Cortical plate	13.37	6.27	20.96	<Quarter
Gyrus rectus	Cortical plate	13.77	3.47	25.09	<Quarter
Superior frontal gyrus	Cortical plate	14.34	8.94	20.00	<Quarter
Cingulate gyrus	Cortical plate	14.99	9.46	20.81	<Quarter
Cuneus	Cortical plate	17.52	7.35	28.65	<Quarter
Precuneus	Cortical plate	17.93	12.34	23.81	<Quarter
Lingual gyrus	Cortical plate	18.51	9.82	27.90	<Quarter
Paracentral lobule	Cortical plate	19.13	13.01	25.57	<Quarter
Insula	Cortical plate	21.81	14.37	29.74	<Quarter

Table 4 Significant differences in volume increase between neighboring regions of CP (or SP) during the early prenatal period (<25.5 GW)

Period	Compartment	Pairs of neighboring regions	Difference in volume increase (%)	95% CI (min, max)		Adjusted *P*-value*
Early	Cortical plate	Superior frontal gyrus:precental gyrus	−10.85	−15.65	−5.78	0.04
Early	Subplate	Insula:parahippocampal gyrus	−34.68	−41.14	−27.51	0.00
Early	Subplate	Paracentral gyrus:cingulate gyrus	−23.15	−28.21	−17.74	0.00
Early	Subplate	Superior frontal gyrus:cingulate gyrus	−23.51	−29.55	−17.03	0.00
Early	Subplate	Pericalcarine cortex:parahippocampal gyrus	−29.17	−35.45	−22.27	0.00
Early	Subplate	Latero-inferior temporal cortex:parahippocampal gyrus	−29.27	−37.78	−19.61	0.00
Early	Subplate	Inferior parietal cortex: latero-inferior temporal cortex	−11.50	−16.04	−6.72	0.01
Early	Subplate	Superior parietal lobule:cuneus	−16.11	−22.44	−9.26	0.02
Early	Subplate	Precuneus:cingulate gyrus	−14.49	−20.46	−8.07	0.03
Early	Subplate	Superior temporal gyrus:latero-inferior temporal cortex	−10.99	−15.77	−5.94	0.04

* *P*-values were adjusted using the Holm procedure.

from (Hill et al. 2010) according to which the regions that expand faster during the early preterm period are regions that mature earlier, that is, expand slower after birth (Hill et al. 2010). Our results also showed faster growth of regions that were suggested to be a human evolutionary gain (lateral temporal cortex, and inferior parietal cortex (Thier and Karnath 1997; Karnath 2001; Vanduffel et al. 2002; Hill et al. 2010)). We observed these differences during early and mid-prenatal periods, that is, periods when cortical maturation is predominantly genetically orchestrated (Kang et al. 2011). Thus, these regional differences in growth rate could potentially underlie the development of species-specific brain functions. For example, compared to other species, the expansion in size of the dorsolateral prefrontal cortex and posterior parietal cortex observed in humans has been suggested to underlie advanced cognitive abilities (e.g., perception, language, reasoning (Geschwind and Rakic 2013)). Furthermore, there are significant differences between humans and monkeys in the function of the parietal cortex, which has been explained by an adaptation of this region during the evolution (Thier and Karnath 1997; Simon et al. 2002). This adaptation most likely resulted in better implementation of human-specific abilities served by the posterior parietal cortex, for example, excellent motion-dependent three-dimensional reconstruction (Vanduffel et al. 2002).

In light of this, we suggest that in the future the differences in prenatal growth and maturation of cortex between primates should be addressed by taking into consideration the developmental periods. A few studies have identified the alteration of several genetically determined developmental events during specific prenatal periods and have suggested that these

Table 5 Significant differences in volume increase between neighboring regions of CP (or SP) during the mid-prenatal period (25.5–31.6 GW)

Period	Compartment	Pairs of neighboring regions	Difference in volume increase (%)	95% CI (min, max)		Adjusted P-value*
Mid-prenatal	Cortical plate	Lateral occipital cortex:inferior parietal cortex	−21.28	−27.34	−14.70	0.00
Mid-prenatal	Cortical plate	Superior parietal lobule:inferior parietal cortex	−21.44	−28.26	−13.96	0.00
Mid-prenatal	Cortical plate	Superior temporal gyrus:inferior parietal cortex	−18.36	−24.69	−11.51	0.01
Mid-prenatal	Cortical plate	Lateral occipital cortex:latero-inferior temporal cortex	−10.75	−15.12	−6.16	0.03
Mid-prenatal	Cortical plate	Precuneus:paracentral lobule	−17.70	−24.77	−9.96	0.05
Mid-prenatal	Subplate	Precuneus:pericalcarine cortex	−30.56	−40.66	−18.73	0.03
Mid-prenatal	Subplate	Superior temporal gyrus:inferior parietal cortex	−11.47	−30.69	−13.27	0.03
Mid-prenatal	Subplate	Latero-inferior temporal cortex:inferior parietal cortex	−18.85	−26.09	−10.90	0.03

* P-values were adjusted using the Holm procedure.

alterations may underlie certain human-specific neurocognitive diseases (Zhu et al. 2018). However, imaging biomarkers of such alterations are yet to be identified in large-scale studies.

During Early and Mid-prenatal Periods the Asynchronous Growth of CP and SP Regions Can Be Detected Even between Neighboring Regions

Our results also indicate that the variation in the relative regional growth rate of the CP and SP can be detected even between neighboring regions. This is evident only during the early and mid-prenatal periods. We explain these findings by spatiotemporal differences in the intensity of histogenic events that could be detected even between neighboring gyral regions.

The CP neurons during mid- and late prenatal periods mature as the volume of their soma increases, so as their dendritic branching (Mrzljak et al. 1988). Furthermore, this neuronal maturation is also governed by differential gene expression across cortical areas (Mackarehtschian et al. 1999; Rubenstein et al. 1999; Bishop et al. 2000). The mid- and late prenatal periods are also characterized by axonal ingrowth of thalamocortical and cortico-cortical fibers in the CP (Blakemore and Molnár 1990; Hevner 2000; Krsnik et al. 2017), appearance of the synaptic spines, and synaptogenesis (Huttenlocher 1979; Huttenlocher and Dabholkar 1997; Petanjek et al. 2009), all of which were suggested to have a role in refinements of gene regulatory networks (Ghosh et al. 1990; Callaway and Borrell 2011; Barber et al. 2015).

Similar to the CP, during the early prenatal period the SP zone contains radially migrating neurons (I. Kostovic and Rakic 1990) and also an abundant extracellular matrix (Allendoerfer and Shatz 1994; Miller et al. 2014; Bakken et al. 2016; Molnár and Hoerder-Suabedissen 2016). During the early and mid-prenatal period, the SP is composed of interstitial neurons (Judaš et al. 2010; Sedmak and Judaš 2019) that are predominantly GABAergic (Back et al. 2001; Rakic and Zecevic 2003; Qu et al. 2016), migrating glial cells (Kostović et al. 2018), and an increasing amount of thalamocortical and cortico-cortical axons that "wait" for an extended period before relocating to the CP (Shatz 1992; Molnár et al. 2003; Molnár and Hoerder-Suabedissen 2016; Krsnik et al. 2017; Alzu'bi et al. 2019). The SP also plays an essential role in the cortical maturation and the formation of local thalamocortical connections, as demonstrated by the experimental ablation of the SP (Ghosh et al. 1990). Furthermore, similar to rodents (Caviness Jr and Frost 1980; Molnár et al. 2003), the density, modality, and time of arrival of thalamocortical axons in the SP and CP most likely vary significantly across cortical regions (Toulmin et al. 2015; Krsnik et al. 2017). Thus, the spatiotemporal differences in volume expansion of the CP and SP that we found between neighboring regions may correspond to spatiotemporal differences in neuronal maturation, dendritic arborization, and the arrival of thalamocortical and cortico-cortical axons during early and mid-prenatal periods. If this is the case, the differential growth of neighboring CP and SP regions during early and mid-prenatal periods would suggest an important role of thalamocortical fibers in areal patterning of the cortex, which is in agreement with the protocortex hypothesis. Lastly, this differential growth of CP and SP could potentially explain the intersubject variation in the size of multimodal associative areas and therefore most likely some variation in the cognitive abilities between individuals (Reardon et al. 2018; Wei et al. 2019).

Asynchronous Growth of CP and SP, Which Occurs during the Emergence of First Sulci and Gyri, Could Drive Cortical Folding of Certain Regions

Finally, we have observed significant differences in the relative growth of neighboring regions of the CP and SP during the early and mid-prenatal periods. During the prenatal development, the thickness of the CP, composed of densely packed post-migratory neurons, changes minimally, while its surface area grows exponentially (Vasung et al. 2016). The early and mid-prenatal periods are also characterized by an increase in the volume of the "water-rich" SP (Kostovic and Rakic 1990; Vasung et al. 2016). However, in contrast to the CP, the SP thickness and the areal variation of the SP thickness increase dramatically during the early and mid-prenatal periods (I. Kostovic and Rakic 1990; Vasung et al. 2016). Based on our results, we hypothesize that the rapid tangential growth of the CP and radial expansion of the SP could partially explain emerging cortical folds. A

recently proposed differential tangential expansion hypothesis suggests that differences in tangential expansion of the layer (i.e., increase in the surface area) result in a local increase of the tangential pressure (Ronan and Fletcher 2015). As the tangential pressure builds, it starts to dissipate by buckling of that expanding layer (Ronan and Fletcher 2015). Our results show that differences between the growth of neighboring regions are predominantly found in SP during the early preterm period. Thus it is possible that differential growth between neighboring regions of the SP, which is characterized by soft gel consistency, induces local tangential force peaks which are relieved by buckling (emergence of sulcal pits identified on SP surfaces (Régis et al. 2005; Lohmann et al. 2008; Yun et al. 2018)). The increase in buckling could lead to an increase in variation of SP thickness (thinner below sulci, thicker below gyri (I. Kostovic and Rakic 1990)) accommodating different tangential growth rates of CP regions. During the mid-prenatal period, the differences in growth rate between neighboring regions can be observed in CP as well as SP. Given that this is a period when majority of primary sulci have already emerged (Chi et al. 1977; Habas et al. 2012), the differences in tangential and radial expansion of the SP and CP could lay down the foundation for emergence of late-appearing primary and some secondary sulci (e.g., intraparietal sulcus that emerges around 26 GW, lateral occipital sulcus that emerges around 26 GW (Chi et al. 1977)).

Numerous computational and animal models were developed in order to test different gyrification hypotheses (for recent reviews see (Borrell 2018; Kroenke and Bayly 2018)). However, none of them take into account all the histogenic events that occur specifically during human brain development. Our study, similar to many others, does not take into account the role of proliferative zones, fetal white matter, establishment and pruning of axonal connections, and radial tension of perforating blood vessels in the establishment of the first cortical folds. Rather, it shows regional differences in the growth rate of CP and SP during early and mid-prenatal periods. Given that the SP represents the largest transient compartment of the neocortical anlage in humans (Judaš 2011), we suggest that the differential growth of SP and CP might play a role in gyrification of the human brain. Thus, different mechanistic theories should take into account differential growth of transient cortical compartments, in particular when describing gyrification that occurs during human fetal brain development.

The Late Prenatal Period Is Characterized by Synchronized Growth of CP

In contrast to the asynchronous growth of CP regions during the early and mid-prenatal periods, we observed synchronous growth of CP regions during the late prenatal period. These results go hand in hand with the temporal "hourglass" model of cortical maturation (Pletikos et al. 2014). According to the hourglass model of cortical maturation, the most striking differences in gene expressions between cortical regions are found during the first two trimesters. During the third trimester, however, the region-specific genes are silenced, except for genes that spur connections between cortical regions (Pletikos et al. 2014).

Limitations

This study has several limitations. We acknowledge that, although we invested major effort to manually correct segmentations, there might be small errors in the parcellation of cortical regions. This is because of the following reasons: (i) inter-individual differences in sulcal root emergence during the early phase of prenatal development could lead to underestimation or overestimation of the volume in certain regions, and (ii) due to the scarcity of sulcal roots (e.g., frontal pole), the delimitation of certain regions was based on the visibility of the fetal cortex in six anatomical views (anterior, posterior, dorsal, dorsolateral, medial, and ventral). In order to minimize these limitations, we reconstructed pial surfaces in the same reference space and employed a rigorous correction for multiple comparisons for all statistical analyses.

Next, although the CP and SP were initially automatically segmented (Gholipour et al. 2017; Vasung et al. 2019), the small errors in segmentation were manually corrected by one reader according to anatomical landmarks that were previously described (Vasung et al. 2019). The reader (L.V.) was blind to age, sex, and hemisphere, and each group of subjects contained at least 10 brains. Thus, although we did not test the intra-rater or inter-rater agreement, we argue that the size of these segmentation errors, in combination with the extensive experience of the reader and a simple morphology of the fetal brain, would be minimal.

Additionally, it is possible that our methods lack the precision to detect subtle differences in regional volume growth. While the gyral parcellation is widely used, it should be noted that this landmark-based gyral cortical map does not reflect the architectural map of the cortex (VOGT and C 1919). Rather, it can only serve as its proxy. Having this in mind, we acknowledge that we most likely missed detecting more subtle changes in volume, which could be detected by voxel-based morphometry or vertex-wise approaches. However, the methodology that would address these differences in fetal brains is under development and currently not available.

Lastly, despite the advances in technology and the development of numerous histology-based brain atlases (Amunts et al. 2013), there is a paucity of information about the cellular density in the cortical regions of the human adult and fetal brain. Consequently, it is difficult to estimate the volume fractions of a particular cortical region that are occupied by cell bodies, neuropil, or extracellular matrix. For this reason, we used some basic principles of developmental neuroscience to interpret our results.

Conclusion

In conclusion, we failed to find significant differences in relative volumes of the CP or of the SP between periods. This is in agreement with the protomap hypothesis (much of the area's destiny/size is determined early during prenatal development). However, we found significant differences in growth rates between certain neighboring regions during early and mid-prenatal periods. This asynchronous growth of CP and SP regions was followed by the synchronous growth of CP during the late prenatal period. Together, these results are in agreement with the protocortex hypothesis. Moreover, the apparent contradiction between these results could be explained by the greater precision within the period analysis. In summary, our results suggest that although the regional CP or SP destiny is predominantly determined early during development, it is fine-tuned during the early and mid-prenatal periods, when peak thalamocortical growth and gyrification occur.

Funding

Ralph Schlaeger Foundation in Neuroradiology; National Institute of Neurological Disorders and Stroke of the National Institutes of Health (award number K23NS101120); American Academy of Neurology Clinical Research Training Fellowship; National Alliance for Research on Schizophrenia & Depression Young Investigator Award from the Brain and Behavior Foundation; National Institutes of Health (grants R01EB018988, R01NS106030, and R01EB013248); Technological Innovations in Neuroscience Award from the McKnight Foundation.

Supplementary Material

Supplementary material is available at *Cerebral Cortex* online.

Acknowledgments

We thank Claude Lepage for technical assistance with the MRI processing pipeline. The content is solely the responsibility of the authors and does not necessarily represent the official views of the National Institutes of Health, Ralph Schlaeger Foundation, or the McKnight Foundation. *Conflict of Interest*: None declared.

References

Allendoerfer KL, Shatz CJ. 1994. The subplate, a transient neocortical structure: its role in the development of connections between thalamus and cortex. *Annual Review of Neuroscience*. 17:185–218.

Alzu'bi A, Homman-Ludiye J, Bourne JA, Clowry GJ. 2019. Thalamocortical afferents innervate the cortical subplate much earlier in development in primate than in rodent. *Cerebral Cortex*. 29:1706–1718.

Amunts K, Lepage C, Borgeat L, Mohlberg H, Dickscheid T, Rousseau M-É, Bludau S, Bazin P-L, Lewis LB, Oros-Peusquens A-M *et al*. 2013. BigBrain: an ultrahigh-resolution 3D human brain model. *Science*. 340:1472–1475.

Amunts K, Zilles K. 2015. Architectonic mapping of the human brain beyond Brodmann. *Neuron*. 88:1086–1107.

Amunts K, Schleicher A, Bürgel U, Mohlberg H, Uylings HB, Zilles K. 1999. Broca's region revisited: Cytoarchitecture and Intersubject variability. *The Journal of Comparative Neurology*. 412:319–341.

Avants BB, Tustison NJ, Song G, Cook PA, Klein A, Gee JC. 2011. A reproducible evaluation of ANTs similarity metric performance in brain image registration. *NeuroImage*. 54:2033–2044.

Back SA, Luo NL, Borenstein NS, Levine JM, Volpe JJ, Kinney HC. 2001. Late Oligodendrocyte progenitors coincide with the developmental window of vulnerability for human perinatal white matter injury. *The Journal of Neuroscience: The Official Journal of the Society for Neuroscience*. 21:1302–1312.

Bakken TE, Miller JA, Ding S-L, Sunkin SM, Smith KA, Ng L, Szafer A, Dalley RA, Royall JJ, Lemon T *et al*. 2016. A comprehensive transcriptional map of primate brain development. *Nature*. 535:367–375.

Barber M, Arai Y, Morishita Y, Vigier L, Causeret F, Borello U, Ledonne F, Coppola E, Contremoulins V, Pfrieger FW *et al*. 2015. Migration speed of Cajal-Retzius cells modulated by vesicular trafficking controls the size of higher-order cortical areas. *Current Biology: CB*. 25:2466–2478.

Bayatti N, Sarma S, Shaw C, Eyre JA, Vouyiouklis DA, Lindsay S, Clowry GJ. 2008. Progressive loss of PAX6, TBR2, NEUROD and TBR1 mRNA gradients correlates with translocation of EMX2 to the cortical plate during human cortical development. *The European Journal of Neuroscience*. 28:1449–1456.

Bayer SA, Altman J. 2005. *The Human Brain during the Second Trimester (Atlas of the Human Central Nervous System Development)*. Indianapolis: CRC Press.

Bayer SA, Altman J. 2007. *The Human Brain during the Early First Trimester*. CRC Press. Boca Raton.

Benjamini Y, Yekutieli D. 2001. The control of the false discovery rate in multiple testing under dependency. *Annals of Statistics*. 29:1165–1188.

Bishop KM, Goudreau G, O'Leary DD. 2000. Regulation of area identity in the mammalian Neocortex by Emx2 and Pax6. *Science*. 288:344–349.

Blakemore C, Molnár Z. 1990. Factors involved in the establishment of specific interconnections between thalamus and cerebral cortex. *Cold Spring Harbor Symposia on Quantitative Biology*. 55:491–504.

Borrell V. 2018. How cells fold the cerebral cortex. *The Journal of Neuroscience: The Official Journal of the Society for Neuroscience*. 38:776–783.

Brodmann K. 1909. *Vergleichende Lokalisationslehre Der Grosshirnrinde in Ihren Prinzipien Dargestellt Auf Grund Des Zellenbaues*. Barth. Leipzig.

Bystron I, Blakemore C, Rakic P. 2008. Development of the human cerebral cortex: boulder committee revisited. *Nature Reviews. Neuroscience*. 9:110–122.

Cadwell CR, Bhaduri A, Mostajo-Radji MA, Keefe MG, Nowakowski TJ. 2019. Development and Arealization of the cerebral cortex. *Neuron*. 103:980–1004.

Callaway EM, Borrell V. 2011. Developmental sculpting of dendritic morphology of layer 4 neurons in visual cortex: influence of retinal input. *The Journal of Neuroscience: The Official Journal of the Society for Neuroscience*. 31:7456–7470.

Caviness VS Jr, Frost DO. 1980. Tangential Organization of Thalamic Projections to the Neocortex in the mouse. *The Journal of Comparative Neurology*. 194:335–367.

Chenn A, Walsh CA. 2002. Regulation of cerebral cortical size by control of cell cycle exit in neural precursors. *Science*. 297:365–369.

Chi JG, Dooling EC, Gilles FH. 1977. Gyral development of the human brain. *Annals of Neurology*. 1:86–93.

Clowry G, Molnár Z, Rakic P. 2010. Renewed focus on the developing human Neocortex. *Journal of Anatomy*. 217:276–288.

Creutzfeldt OD. 1977. Generality of the functional structure of the Neocortex. *Die Naturwissenschaften*. 64:507–517.

Defelipe J, González-Albo MC, Del Río MR, Elston GN. 1999. Distribution and patterns of connectivity of interneurons containing Calbindin, Calretinin, and Parvalbumin in visual areas of the occipital and temporal lobes of the macaque monkey. *The Journal of Comparative Neurology*. 412: 515–526.

Desikan RS, Ségonne F, Fischl B, Quinn BT, Dickerson BC, Blacker D, Buckner RL, Dale AM, Maguire RP, Hyman BT *et al*. 2006. An automated Labeling system for subdividing the human cerebral cortex on MRI scans into Gyral based regions of interest. *NeuroImage*. 31:968–980.

Diogo MC, Prayer D, Gruber GM, Brugger PC, Stuhr F, Weber M, Bettelheim D, Kasprian G. 2019. Echo-planar FLAIR sequence improves subplate visualization in Fetal MRI of the brain. *Radiology*. 292:159–169.

Donkelaar HJ T, Tzourio-Mazoyer N, Mai JK. 2018. Toward a common terminology for the Gyri and sulci of the human cerebral cortex. *Frontiers in Neuroanatomy*. 12:93. doi: 10.3389/fnana.2018.00093.

Ducharme S, Albaugh MD, Nguyen T-V, Hudziak JJ, Mateos-Pérez JM, Labbe A, Evans AC, Karama S, Brain Development Cooperative Group. 2016. Trajectories of cortical thickness maturation in normal brain development–the importance of quality control procedures. *NeuroImage*. 125:267–279.

Economo CF v, Koskinas GN. 1925. Die Cytoarchitektonik Der Hirnrinde des Erwachsenen menschen. *Berlin: Springer*.

Eickhoff SB, Stephan KE, Mohlberg H, Christian Grefkes GRF, Amunts K, Zilles K. 2005. A new SPM toolbox for combining probabilistic Cytoarchitectonic maps and functional imaging data. *NeuroImage*. 25:1325–1335.

Elston GN, Benavides-Piccione R, DeFelipe J. 2001. The pyramidal cell in cognition: a comparative study in human and monkey. *The Journal of Neuroscience: The Official Journal of the Society for Neuroscience*. 21:RC163.

Garel C, Chantrel E, Brisse H, Elmaleh M, Luton D, Oury JF, Sebag G, Hassan M. 2001. Fetal cerebral cortex: normal gestational landmarks identified using prenatal MR imaging. *AJNR. American Journal of Neuroradiology*. 22:184–189.

Germann J, Robbins S, Halsband U, Petrides M. 2005. Precentral Sulcal complex of the human brain: morphology and statistical probability maps. *The Journal of Comparative Neurology*. 493:334–356.

Geschwind DH, Rakic P. 2013. Cortical evolution: judge the brain by its cover. *Neuron*. 80:633–647.

Gholipour A, Estroff JA, Barnewolt CE, Robertson RL, Ellen Grant P, Gagoski B, Warfield SK, Afacan O, Connolly SA, Neil JJ *et al*. 2014. Fetal MRI: a technical update with educational aspirations. *Concepts in Magnetic Resonance. Part A. Bridging Education and Research*. 43:237–266.

Gholipour A, Rollins CK, Velasco-Annis C, Ouaalam A, Akhondi-Asl A, Afacan O, Ortinau CM, Clancy S, Limperopoulos C, Yang E *et al*. 2017. A normative spatiotemporal MRI atlas of the Fetal brain for automatic segmentation and analysis of early brain growth. *Scientific Reports*. 7:476.

Ghosh A, Antonini A, McConnell SK, Shatz CJ. 1990. Requirement for subplate neurons in the formation of Thalamocortical connections. *Nature*. 347:179–181.

Habas PA, Scott JA, Roosta A, Rajagopalan V, Kim K, Francois R, James Barkovich A, Glenn OA, Studholme C. 2012. Early folding patterns and asymmetries of the normal human brain detected from in utero MRI. *Cerebral Cortex*. 22:13–25.

Hawrylycz MJ, Ed SL, Guillozet-Bongaarts AL, Shen EH, Ng L, Miller JA, van de LN, Smith KA, Ebbert A, Riley ZL *et al*. 2012. An anatomically comprehensive atlas of the adult human brain Transcriptome. *Nature*. 489:391–399.

Hevner RF. 2000. Development of connections in the human visual system during Fetal mid-gestation: a DiI-tracing study. *Journal of Neuropathology and Experimental Neurology*. 59:385–392.

Hill J, Inder T, Neil J, Dierker D, Harwell J, Van Essen D. 2010. Similar patterns of cortical expansion during human development and evolution. *Proceedings of the National Academy of Sciences of the United States of America*. 107:13135–13140.

Holland PW, Welsch RE. 1977. Robust regression using iteratively reweighted least-squares. *Communications in Statistics - Theory and Methods*. 6:813–827.

Holm S. 1979. A simple sequentially Rejective multiple test procedure. *Scandinavian Journal of Statistics, Theory and Applications*. 6:65–70.

Huttenlocher PR. 1979. Synaptic density in human frontal cortex - developmental changes and effects of aging. *Brain Research*. 163:195–205.

Huttenlocher PR, Dabholkar AS. 1997. Regional differences in synaptogenesis in human cerebral cortex. *The Journal of Comparative Neurology*. 387:167–178.

Iaria G, Petrides M. 2007. Occipital sulci of the human brain: variability and probability maps. *The Journal of Comparative Neurology*. 501:243–259.

Judaš M. 2011. Prenatal Development of the Human Fetal Telencephalon. In: Prayer D, editor. *Fetal MRI*. Berlin, Heidelberg: Springer Berlin Heidelberg, pp. 81–146.

Judaš, Miloš, Maja Cepanec, and Ivica Kostović. 2006. Prenatal and Postnatal Development of Human Fronto-Opercular Cerebral Cortex. In: 5th Forum of European Neuroscience. bib.irb.hr. https://bib.irb.hr/prikazi-rad?rad=253134.

Judaš M, Sedmak G, Pletikos M, Jovanov-Milošević N. 2010. Populations of subplate and interstitial neurons in Fetal and adult human telencephalon. *Journal of Anatomy*. 217:381–399.

Kainz B, Steinberger M, Wein W, Kuklisova-Murgasova M, Malamateniou C, Keraudren K, Torsney-Weir T, Rutherford M, Aljabar P, Joseph V *et al*. 2015. Fast volume reconstruction from motion corrupted stacks of 2D slices. *IEEE Transactions on Medical Imaging*. 34:1901–1913.

Kang HJ, Kawasawa YI, Cheng F, Zhu Y, Xuming X, Li M, Sousa AMM, Pletikos M, Meyer KA, Sedmak G *et al*. 2011. Spatio-temporal Transcriptome of the human brain. *Nature*. 478:483–489.

Karlen SJ, Krubitzer L. 2009. Effects of bilateral Enucleation on the size of visual and nonvisual areas of the brain. *Cerebral Cortex*. 19:1360–1371.

Karnath HO. 2001. New insights into the functions of the superior temporal cortex. *Nature Reviews. Neuroscience*. 2:568–576.

Khundrakpam BS, Tohka J, Evans AC, Brain Development Cooperative Group. 2015. Prediction of brain maturity based on cortical thickness at different spatial resolutions. *NeuroImage*. 111:350–359.

Kostovic I, Rakic P. 1990. Developmental history of the transient subplate zone in the visual and somatosensory cortex of the macaque monkey and human brain. *The Journal of Comparative Neurology*. 297:441–470.

Kostović I, Išasegi IŽ, Krsnik Ž. 2018. Sublaminar Organization of the Human Subplate: developmental changes in the distribution of neurons, glia, growing axons and extracellular matrix. *Journal of Anatomy*. 235:481–506. doi: 10.1111/joa.12920.

Kostović I, Judaš M, Petanjek Z. 2008a. *Structural Development of the Human Prefrontal Cortex*. Handbook of Developmental Cognitive Neuroscience: MIT Press.

Kostović I, Judas M, Rados M, Hrabac P. 2002. Laminar Organization of the Human Fetal Cerebrum Revealed by Histochemical markers and magnetic resonance imaging. *Cerebral Cortex*. 12:536–544.

Kostovic I, Vasung L. 2009. Insights from in vitro Fetal magnetic resonance imaging of cerebral development. *Seminars in Perinatology*. 33:220–233.

Kostović, Ivica, Lana Vasung, Milan Radoš, Marko Čuljat, David Ozretić, Miloš Judaš, and Marko Radoš. 2008b. Early Lamination of the Cortical Plate in the Prefrontal Cortex of the Human Fetus: In Vitro 3T MR Imaging and Histological

Analysis. In Neuroscience 2008. bib.irb.hr. https://bib.irb.hr/prikazi-rad?rad=398776.
Kroenke CD, Bayly PV. 2018. How forces fold the cerebral cortex. *The Journal of Neuroscience: The Official Journal of the Society for Neuroscience*. 38:767–775.
Krsnik Ž, Majić V, Vasung L, Huang H, Kostović I. 2017. Growth of Thalamocortical Fibers to the somatosensory cortex in the human Fetal brain. *Frontiers in Neuroscience*. 11:233.
Lohmann G, Yves von Cramon D, Colchester ACF. 2008. Deep Sulcal landmarks provide an organizing framework for human cortical folding. *Cerebral Cortex*. 18:1415–1420.
Lyall AE, Shi F, Geng X, Woolson S, Li G, Wang L, Hamer RM, Shen D, Gilmore JH. 2015. Dynamic development of regional cortical thickness and surface area in early childhood. *Cerebral Cortex*. 25:2204–2212.
Mackarehtschian K, Lau CK, Caras I, McConnell SK. 1999. Regional differences in the developing cerebral cortex revealed by Ephrin-A5 expression. *Cerebral Cortex*. 9: 601–610.
Mallamaci A, Stoykova A. 2006. Gene networks controlling early cerebral cortex Arealization. *The European Journal of Neuroscience*. 23:847–856.
Meyer G. 2007. Genetic control of neuronal migrations in human cortical development. *Advances in Anatomy, Embryology, and Cell Biology*. 189:1–111.
Miller JA, Song-Lin Ding SM, Sunkin KAS, Ng L, Szafer A, Ebbert A, Riley ZL, Royall JJ, Aiona K *et al*. 2014. Transcriptional landscape of the prenatal human brain. *Nature*. 508:199–206.
Molnár Z, Higashi S, López-Bendito G. 2003. Choreography of early Thalamocortical development. *Cerebral Cortex*. 13:661–669.
Molnár Z, Hoerder-Suabedissen A. 2016. Regional Scattering of Primate Subplate. In: *Proceedings of the National Academy of Sciences of the United States of America*. 113:9676–9678.
Mrzljak L, Uylings HB, Kostovic I, Van Eden CG. 1988. Prenatal development of neurons in the human prefrontal cortex: I. a qualitative Golgi study. *The Journal of Comparative Neurology*. 271:355–386.
O'Leary DD. 1989. Do cortical areas emerge from a Protocortex? *Trends in Neurosciences*. 12:400–406.
O'Leary DDM, Nakagawa Y. 2002. Patterning Centers, regulatory genes and extrinsic mechanisms controlling Arealization of the Neocortex. *Current Opinion in Neurobiology*. 12: 14–25.
Ono M, Kubik S, Abernathey CD, Yaşargil MG. 1990. *Atlas of the Cerebral Sulci*. Vol 6. Stuttgart: Georg Thieme Verlag.
Palomero-Gallagher N, Zilles K. 2018. Cyto- and receptor architectonic mapping of the human brain. *Handbook of Clinical Neurology*. 150:355–387.
Paredes MF, James D, Gil-Perotin S, Kim H, Cotter JA, Ng C, Sandoval K, Rowitch DH, Xu D, McQuillen PS *et al*. 2016. Extensive migration of young neurons into the infant human frontal lobe. *Science*. 354. doi: 10.1126/science.aaf7073.
Petanjek Z, Kostović I, Esclapez M. 2009. Primate-specific origins and migration of cortical GABAergic neurons. *Frontiers in Neuroanatomy*. 3:26.
Pletikos M, Sousa AMM, Sedmak G, Meyer KA, Zhu Y, Cheng F, Li M, Kawasawa YI, Sestan N. 2014. Temporal specification and Bilaterality of human neocortical topographic gene expression. *Neuron*. 81:321–332.
Qu, Ma J, Y-C Y, Fu Y. 2016. Postnatal development of GABAergic interneurons in the neocortical subplate of mice. *Neuroscience*. 322:78–93.
Rados M, Judas M, Kostović I. 2006. In vitro MRI of brain development. *European Journal of Radiology*. 57:187–198.
Rakic P. 1988. Specification of cerebral cortical areas. *Science*. 241:170–176.
Rakic P, Sidman RL. 1968. Supravital DNA synthesis in the developing human and mouse brain. *Journal of Neuropathology and Experimental Neurology*. 27:246–276.
Rakic P, Suñer I, Williams RW. 1991. A novel Cytoarchitectonic area induced experimentally within the primate visual cortex. *Proceedings of the National Academy of Sciences of the United States of America*. 88:2083–2087.
Rakic S, Zecevic N. 2003. Early Oligodendrocyte progenitor cells in the human Fetal telencephalon. *Glia*. 41:117–127.
Raznahan A, Shaw P, Lalonde F, Stockman M, Wallace GL, Greenstein D, Clasen L, Gogtay N, Giedd JN. 2011. How does your cortex grow? *The Journal of Neuroscience: The Official Journal of the Society for Neuroscience*. 31:7174–7177.
Reardon PK, Seidlitz J, Vandekar S, Liu S, Patel R, Park MTM, Alexander-Bloch A, Clasen LS, Blumenthal JD, Lalonde FM *et al*. 2018. Normative brain size variation and brain shape diversity in humans. *Science*. 360:1222–1227.
Régis J, Mangin J-F, Ochiai T, Frouin V, Riviére D, Cachia A, Tamura M, Samson Y. 2005. Sulcal root' generic model: a hypothesis to overcome the variability of the human cortex folding patterns. *Neurologia Medico-Chirurgica*. 45:1–17.
Ronan L, Fletcher PC. 2015. From genes to folds: a review of cortical Gyrification theory. *Brain Structure & Function*. 220:2475–2483.
Rubenstein JL, Anderson S, Shi L, Miyashita-Lin E, Bulfone A, Hevner R. 1999. Genetic control of cortical regionalization and connectivity. *Cerebral Cortex*. 9(6):524–532.
Rubenstein JL, Rakic P. 1999. Genetic control of cortical development. *Cerebral Cortex*. 9:521–523.
Rubenstein JL, Shimamura K, Martinez S, Puelles L. 1998. Regionalization of the Prosencephalic neural plate. *Annual Review of Neuroscience*. 21:445–477.
Salehi M, Sadegh S, Erdogmus D, Gholipour A. 2017. Auto-context convolutional neural network (auto-net) for brain extraction in magnetic resonance imaging. *IEEE Transactions on Medical Imaging*. 36:2319–2330.
Sanides F. 1964. The Cyto-Myeloarchitecture of the human frontal lobe and its relation to phylogenetic differentiation of the cerebral cortex. *Journal Fur Hirnforschung*. 7: 269–282.
Schleicher A, Amunts K, Geyer S, Kowalski T, Schormann T, Palomero-Gallagher N, Zilles K. 2000. A stereological approach to human cortical architecture: identification and delineation of cortical areas. *Journal of Chemical Neuroanatomy*. 20:31–47.
Sedmak G, Judaš M. 2019. The Total number of white matter interstitial neurons in the human brain. *Journal of Anatomy*. 235:626–636.
Segal E, Petrides M. 2012. The morphology and variability of the caudal rami of the superior temporal sulcus. *The European Journal of Neuroscience*. 36:2035–2053.
Shatz CJ. 1992. How are specific connections formed between thalamus and cortex? *Current Opinion in Neurobiology*. 2: 78–82.
Shaw P, Kabani NJ, Lerch JP, Eckstrand K, Lenroot R, Gogtay N, Greenstein D, Evans A, Rapoport JL, Giedd JN *et al*. 2008. Neurodevelopmental trajectories of the human cerebral cortex. *The Journal of Neuroscience: The Official Journal of the Society for Neuroscience*. 28:3586–3594.

Simon O, Mangin JF, Cohen L, Le Bihan D, Dehaene S. 2002. Topographical layout of hand, eye, calculation, and language-related areas in the human parietal lobe. *Neuron*. 33:475–487.

Smiley JF, Levey AI, Ciliax BJ, Goldman-Rakic PS. 1994. D1 dopamine receptor Immunoreactivity in human and monkey cerebral cortex: predominant and Extrasynaptic localization in dendritic spines. *Proceedings of the National Academy of Sciences of the United States of America*. 91:5720–5724.

Tamnes CK, Herting MM, Goddings A-L, Meuwese R, Blakemore S-J, Dahl RE, Güroğlu B, Raznahan A, Sowell ER, Crone EA *et al.* 2017. Development of the cerebral cortex across adolescence: a multisample study of inter-related longitudinal changes in cortical volume, surface area, and thickness. *The Journal of Neuroscience: The Official Journal of the Society for Neuroscience*. 37:3402–3412.

Thier P, Karnath H-O. 1997. *Parietal Lobe Contributions to Orientation in 3D Space*. Vol 25. Heidelberg: Springer Verlag.

Thompson PM, Andreassen OA, Arias-Vasquez A, Bearden CE, Boedhoe PS, Brouwer RM, Buckner RL, Buitelaar JK, Bulayeva KB, Cannon DM *et al.* 2017. ENIGMA and the individual: predicting factors that affect the brain in 35 countries worldwide. *NeuroImage*. 145:389–408.

Toga AW, Thompson PM, Sowell ER. 2006. Mapping brain maturation. *Trends in Neurosciences*. 29:148–159.

Toulmin H, Beckmann CF, O'Muircheartaigh J, Ball G, Nongena P, Makropoulos A, Ederies A, Counsell SJ, Kennea N, Arichi T *et al.* 2015. Specialization and integration of functional Thalamocortical connectivity in the human infant. *Proceedings of the National Academy of Sciences of the United States of America*. 112:6485–6490.

Tustison NJ, Avants BB, Cook PA, Zheng Y, Egan A, Yushkevich PA, Gee JC. 2010. N4ITK: improved N3 bias correction. *IEEE Transactions on Medical Imaging*. 29:1310–1320.

Van der H, Woolsey TA. 1973. Somatosensory cortex: structural alterations following early injury to sense organs. *Science*. 179:395–398.

Vanduffel W, Fize D, Peuskens H, Denys K, Sunaert S, Todd JT, Orban GA. 2002. Extracting 3D from motion: differences in human and monkey Intraparietal cortex. *Science*. 298:413–415.

Vasung L, Turk EA, Ferradal SL, Sutin J, Stout JN, Ahtam B, Lin P-Y, Ellen Grant P. 2018. Exploring early human brain development with structural and physiological neuroimaging. *NeuroImage*. 187:226–254. doi: 10.1016/j.neuroimage.2018.07.041.

Vasung L, Lepage C, Radoš M, Pletikos M, Goldman JS, Richiardi J, Raguž M *et al.* 2016. Quantitative and qualitative analysis of transient Fetal compartments during prenatal human brain development. *Frontiers in Neuroanatomy*. 10:11.

Vasung L, Rollins CK, Yun HJ, Velasco-Annis C, Zhang J, Wagstyl K, Evans A, Warfield SK, Feldman HA, Grant PE *et al.* 2019. Quantitative in vivo MRI assessment of structural asymmetries and sexual dimorphism of transient Fetal compartments in the human brain. *Cerebral Cortex*. doi: 10.1093/cercor/bhz200.

VOGT and C. 1919. Allgemeinere Ergebnisse Unserer Hirnforschung. *Journal of Neurology and Psychology (Leipz)*. 25:279–461.

Vogt C, Vogt O. 1926. Die Vergleichend-Architektonische und die Vergleichend-Reizphysiologische Felderung Der Großhirnrinde Unter Besonderer Berücksichtigung Der Menschlichen. *Die Naturwissenschaften*. 14:1190–1194.

Vogt O. 1910. Die Myeloarchitektonische Felderung des Menschlichen Stirnhirns. *Journal of Neurology and Psychology*. 15:221–232.

Wei Y, de Lange SC, Scholtens LH, Watanabe K, Ardesch DJ, Jansen PR, Savage JE, Li L, Preuss TM, Rilling JK *et al.* 2019. Genetic mapping and evolutionary analysis of human-expanded cognitive networks. *Nature Communications*. 10:4839.

Workman AD, Charvet CJ, Clancy B, Darlington RB, Finlay BL. 2013. Modeling transformations of neurodevelopmental sequences across mammalian species. *The Journal of Neuroscience: The Official Journal of the Society for Neuroscience*. 33:7368–7383.

Xu G, Broadbelt KG, Haynes RL, Folkerth RD, Borenstein NS, Belliveau RA, Trachtenberg FL, Volpe JJ, Kinney HC. 2011. Late development of the GABAergic system in the human cerebral cortex and white matter. *Journal of Neuropathology and Experimental Neurology*. 70:841–858.

Yun HJ, Chung AW, Vasung L, Yang E, Tarui T, Rollins CK, Ortinau CM, Ellen Grant P, Im K. 2018. Automatic Labeling of cortical sulci for the human Fetal brain based on Spatio-temporal information of Gyrification. *NeuroImage*. 188: 473–482.

Zhu Y, Sousa AMM, Gao T, Skarica M, Li M, Santpere G, Esteller-Cucala P, Juan D, Ferrández-Peral L, Gulden FO *et al.* 2018. Spatiotemporal Transcriptomic divergence across human and macaque brain development. *Science*. 362:eaat8077. doi: 10.1126/science.aat8077.

Zilles K, Rehkämper G, Schleicher A. 1979. A quantitative approach to Cytoarchitectonics. V. the areal pattern of the cortex of Microcebus Murinus (E. Geoffroy 1828), (Lemuridae, primates). *Anatomy and Embryology*. 157: 269–289.

Zlatkina V, Petrides M. 2010. Morphological patterns of the Postcentral sulcus in the human brain. *The Journal of Comparative Neurology*. 518:3701–3724.

Išasegi Ž, Iris MR, Krsnik Ž, Radoš M, Benjak V, Kostović I. 2018. Interactive Histogenesis of axonal strata and proliferative zones in the human Fetal Cerebral Wall. *Brain Structure & Function*. 223:3919–3943.